Optical Properties of Injection-Molded Polystyrene Scintillators. II. Distribution of Dopants

J. A. Martins,[1] J. Seixas,[1] M. J. Oliveira,[1] A. Maio,[2,3] A. S. Pouzada[1]

[1]*Departamento de Engenharia de Polímeros, Instituto de Polímeros e Compósitos, Universidade do Minho, Azurém, 4800-058 Guimarães, Portugal*
[2]*Departamento de Física, Universidade de Lisboa, Campo Grande, Edifício C1, 1749–016 Lisboa, Portugal*
[3]*Laboratório de Investigação em Partículas, Av. Elias Garcia 14, 1000–149 Lisboa, Portugal*

Received 16 April 2002; accepted 23 August 2002

ABSTRACT: The distribution of fluorescing dye solutes in scintillating tiles for the Tilecal/Atlas project is assessed, and a link between the homogeneity of the dopant distribution and the optical yield and nonuniformity is established. The effect of the injection-molding parameters on the dye distribution is also analyzed, as well as the actual dye incorporation into the scintillators. This incorporation has been assessed with a set of experiments performed with laboratory samples with controlled amounts of additives and with samples obtained from injection-molded scintillators. Differential scanning calorimetry has been used to characterize the raw material and to establish a link between the thermophysical properties and the processing conditions, and it is proven to be a quite appropriate technique. © 2003 Wiley Periodicals, Inc. J Appl Polym Sci 88: 2714–2718, 2003

Key words: fluorescence; dyes/pigments; differential scanning calorimetry (DSC); polystyrene

INTRODUCTION

In the first part of this series,[1] the effects of the processing conditions on the optical properties of polystyrene (PS) scintillators are analyzed and discussed. The light yield of the scintillators has been shown to be dependent on the molecular orientation induced by the processing conditions frozen-in upon cooling. This frozen-in orientation was indirectly assessed by the birefringence at different points in the scintillator. The results from this part of the work suggested a possible dependence of the scintillator performance on the molecular weight of the polymer and on the distribution of the dopants in the moldings.

According to the Atlas Technical Design Report,[2] the raw material of the scintillators must be PS. The grade to be used must have suitable optical properties, and the dopant solutes are *p*-terphenil (PTP) and 2,2′-*p*-phenilene-bis(5-pheniloxazole) (POPOP). In normal applications of the scintillating tiles, as detectors of ionizing radiation,[3] an ionizing particle induces initial radiation in the PS matrix at wavelengths of 240–300 nm. The radiation that is transmitted through the matrix is absorbed by the PTP and re-emitted. This light, coming from the PTP in the wavelength range of 320–400 nm, is absorbed by the POPOP and re-emitted again in a longer blue wavelength.

A short description of the mechanism of the interaction between the radiation and the scintillator is useful for an understanding of the scintillating process, that is, the role played by the processing conditions and dopant distribution, and is included in the appendix.

Because the absolute scintillation efficiency of a ternary scintillator is directly proportional to the quantum efficiencies of the energy transfer from the main constituent to the most concentrated dopant and from this to the less concentrated dopant, it is expected that they are directly affected by an inhomogeneous distribution of dopants. Therefore, the homogeneity of the dopant distribution is a determining parameter for the light output yield.

The nonuniformity of the optical properties of the scintillators, together with other factors associated with the assembly in the calorimeter and with the reading of the signals from different tiles, contributes to the actual readout. The nonuniformity inside a tile should be below 5% to fulfil the specifications of the Atlas project.[2]

The mold design solution and a nonhomogeneous distribution of dopants are among the factors that may contribute to a poor nonuniformity. In the mold design solution adopted for the production, the location of the only welding line is not critical for the transmission of light along the scintillator. Therefore, the apparent nonuniformity can directly be associated with a nonhomogeneous distribution of the dopants in the moldings. To our knowledge, in the literature[4–6] there is no reference to the influence of the mold design and the processing conditions on the dopant distribution or to how this distribution can be measured.

Correspondence to: J. A. Martins (jamartins@dep.uminho.pt).

Journal of Applied Polymer Science, Vol. 88, 2714–2718 (2003)

TABLE I
Processing Conditions and Main Optical Properties of the Scintillators Used in This Work

	Tile 17	Tile 136
Injection temperature (°C)	185	175
Injection pressure (MPa)	14	15
Back-pressure (MPa)	2	3
Average light output (au)	612	250
Average attenuation length (mm)	578	299

Both scintillators were from the same material BASF 158K.

Results obtained by Swank and Buck in 1953[7] showed that the light output increases with the PTP concentration, attaining a maximum at a concentration between 1 and 2.2 wt %. For POPOP, it was reported from experimental data that its optimal concentration would be 0.05 wt %.[6] These conclusions were confirmed by recent work carried out by Senchishin et al.[4] These investigators also analyzed the role of the solute concentration on the radiation hardness and found that an increase in the concentration of PTP did not affect the radiation hardness, unlike an increase in the POPOP concentration. The roles that different concentrations of dopants might have on the optical yield was discussed,[3,4] but the actual concentration in the injection-molded tiles was not evaluated.

Therefore, the need to establish a reliable and fast method of characterizing the relevant thermophysical properties of the raw material and the distribution of the dopants in the processed tiles appears to be appropriate at this stage. The use of the differential scanning calorimetry (DSC) technique was considered for assessing the relevant thermophysical properties of the material that lead to the determination of the molecular weight of the polymer and to the estimation of the concentration of the dopants in the moldings.

EXPERIMENTAL

Materials

Experimental details concerning the moldings of the PS materials used in this work are described in the first part of this series.[1] For convenience, the most relevant information is repeated in Table I, together with some optical indicators determined therein for the BASF grades.

Thermophysical characterization

The DSC experiments were performed with a PerkinElmer DSC-7 (Norwalk, CT) calibrated with standard metals (indium and lead) at each scanning rate used in the experiments. The purge gas rate was set to the standard value (20 cm^3/min), and the temperature of the cold block was 5°C. For the heat capacity measurements, the three-curve method was used. Sapphire discs were used as reference materials.

The measurements of the glass-transition temperature (T_g) were performed at different heating rates that are listed alongside the data. So that every sample had a thermal history identical to that used in subsequent scans for T_g measurements, all specimens were heated in the differential scanning calorimeter up to 180°C and then cooled down to 30°C at the same scanning rate. The measurements were performed on samples of the original raw materials used in the production of the scintillators, on selected scintillators with different optical properties, and on samples with various but controlled amounts of the dopants, as described next.

For the dependence of T_g on the molecular weight to be ascertained, several gel permeation chromatography (GPC) PS standards, with molecular weights ranging from 5050 to 370,000 g/mol, were analyzed. With the correlation established from these PS standards, an approximate value for the molecular weight of the other raw materials could be derived from the corresponding values of T_g obtained by DSC.

The T_g data were also used to quantify the effective amount of dopants incorporated into the raw material and the homogeneity of their distribution in the scintillators. The need for these data is justified by the fact that, because of the electrostatic charges developed during the mixing stage before the injection molding, a fraction of the dopants adhered to the mixing barrel walls, and they were not actually incorporated into the mixture to be processed.

The preparation of laboratory samples with known (and controlled) amounts of dopants was performed by the dissolution of 10 g of PS pellets in chloroform with the corresponding amounts of the two solutes. The mixture was magnetically stirred at room temperature until the complete dissolution of PS. The stirred solution was then removed, and the solvent evaporated. Samples with concentrations of PTP of 1.5–6% (and the corresponding proportional amounts of POPOP) were prepared and analyzed by DSC.

RESULTS AND DISCUSSION

Figure 1 shows the curves of the specific heat capacity data for all the raw materials used in this work and for two PS standards with molecular weights of 5050 and 370,000 g/mol. The values of T_g obtained for the PS standards versus the respective molecular weights are plotted in Figure 2. All scans corresponding to the data in Figures 1 and 2 were performed at the same scanning rate (10°C/min) after a controlled cooling run at the same rate. From the data shown in these figures, it is possible to infer that these four raw materials have different molecular weights. The poor optical properties of the scintillators produced with the Edistir and BASF 143E grades[1] are probably associated with the relatively lower molecular weights of these grades. From Figure 2, approximate values for the molecular weights of PSM 115 and BASF 158 K of

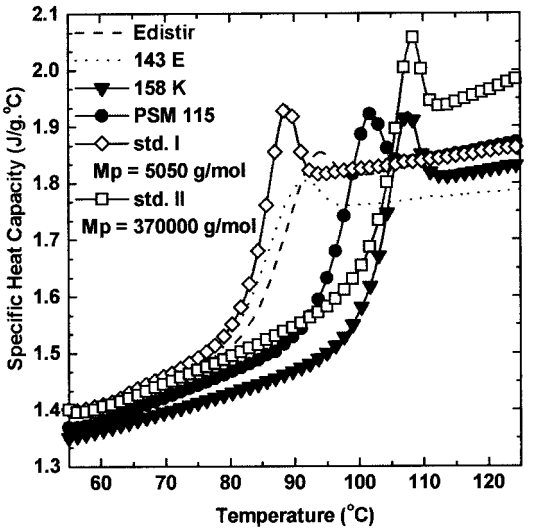

Figure 1 Measurements of the specific heat capacity with respect to a sapphire standard. All scans were performed at 10°C/min after controlled cooling at the same scanning rate. The plot also shows scans performed with two PS samples (GPC standards) with controlled molecular weights.

20,000 and 380,000 g/mol, respectively, are also predictable. The melt-flow rates of these two materials are 13.4 g/600 s and 3 g/600 s, respectively.

The data for T_g of the raw materials and the samples taken from the scintillators are listed in Table II. These samples have lower values of T_g, which may be ascribed to the plasticizing effect of the dopants, as suggested by the results shown in Figure 3(a,b). It must be stressed that the samples of the scintillators used for evaluating T_g were collected from the tiles at a central position near the gate. Because the effect of the processing conditions on T_g was erased by a previous heating at 180°C followed by controlled cooling down to 30°C, in principle, T_g should be nearly the same for every sample of the same material. Therefore, the differences shown in Table II are due to the effect that the processing conditions have on the dispersion

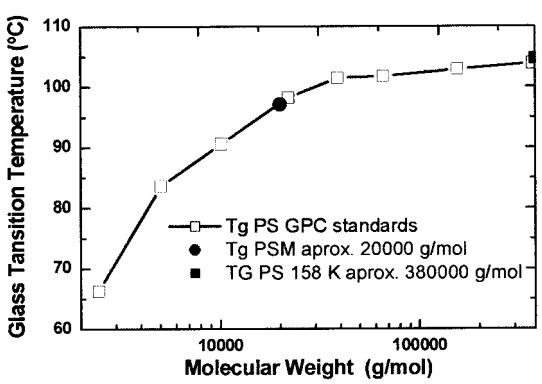

Figure 2 Variation of T_g of PS (GPC standards) with the molecular weight: (●) PSM 115, (■) BASF 158 K, and (□) GPC standards.

TABLE II
T_g's of the Raw Materials and Molded in Scintillators

Raw material	T_g (°C)	Tile	T_g (°C)
PSM 115	96.943	173	90.430
		178	90.138
BASF 158K	104.616	16	98.666
		17	95.560
		130	97.292
		136	96.532

The measurements were performed at a scanning rate of 8°C/min.

of the dopants, which end up with a heterogeneous distribution.

In Figure 3(a,b), the variation of T_g with the scanning rate and concentration of the dopants is shown for PSM 115 and BASF 158K, respectively. The plots confirm the aforementioned evidence of a plasticizing action of the dopants in the polymer used in the tiles. The plasticization effect causes T_g to decrease as the dopant concentration increases.

It is mentioned in the first part of this series[1] that the average light yield and attenuation length of tiles produced under different processing conditions are very different. Because the tiles showing poorer optical

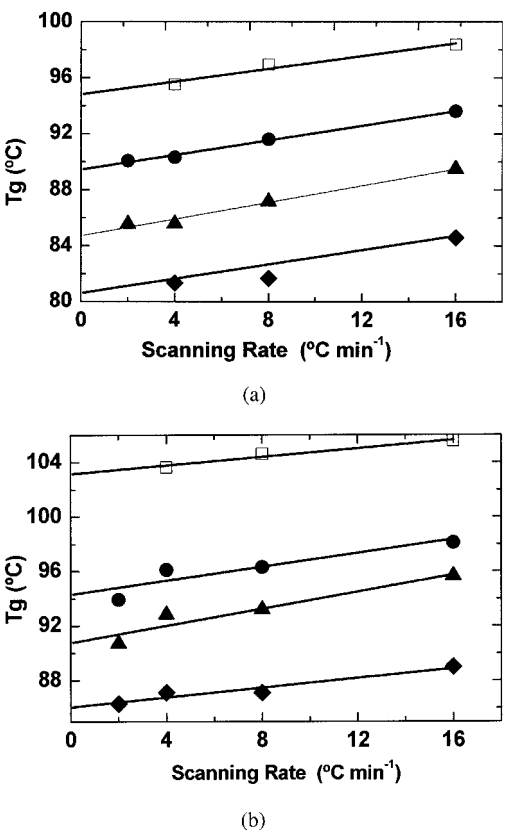

Figure 3 Effect of the dopant concentration and scanning rate on T_g for (a) PSM 115 and (b) BASF 158K: (□) raw material, (●) material with 1.5% PTP and 0.05% POPOP, (▲) material with 3% PTP and 0.1% POPOP, and (♦) material with 6% PTP and 0.2% POPOP.

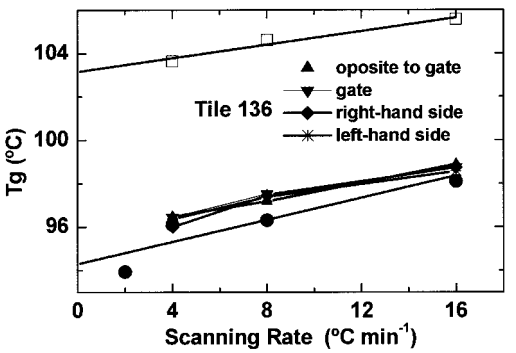

(a)

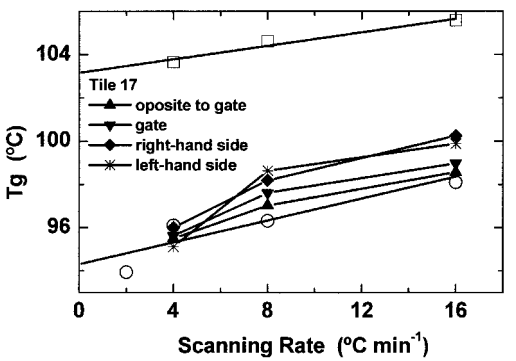

(b)

Figure 4 Variation of T_g with the scanning rate for samples collected at different positions in the scintillators for (a) tile 136 and (b) tile 17: (□) raw material (BASF 158K), (●) material with 1.5% PTP and 0.05% POPOP, (▲) sample extracted from the side opposite to the gate, (▼) sample extracted from the side near the gate, (♦) sample extracted from the right-hand side, and (✳) sample extracted from the left-hand side.

properties also have distinct values of T_g, it appears that not only the variation of birefringence but also the dopant distribution affect the nonuniformity of the light output.

The two top lines in Figure 3(a,b), which correspond to the original material and to the material doped with 1.5% PTP and 0.05% POPOP, respectively, were used as calibration lines to derive the effective incorporation of the dopants and to assess their distribution in the tile. The result of this exercise is shown in Figure 4(a,b) for tiles 136 and 17, respectively, both molded in BASF 158 K. The data obtained for tiles 173 and 178, molded in PSM 115, suggest a behavior similar to that of tile 136. As indicated in the caption of the figure, the specimens were taken from different positions in the tiles.

From the data points corresponding to the specimens taken from the tiles, lying between the 0 and 1.5% PTP calibration lines [see Fig. 4(a,b)], it is possible to conclude that the additives are effectively incorporated in amounts lower than planned. This is caused by the aforementioned adhesion of the dopant particles to the barrel wall during the mixing stage. For tile 136, in Figure 4(a), the distribution of additives is almost uniform, whereas for tile 17, in Figure 4(b), there is a larger scatter in their distribution.

A quantification of the additives incorporated into the tiles, as well as their distribution, may be estimated from a plot of T_g as a function of the true amount of the additives (Fig. 5). With the data obtained at a scanning rate of 8°C/min [Fig. 3(b)], an exponential decay function may be used to describe the observed variation of T_g:

$$T_g = 83.612 + 20.782 \cdot \exp(-x/3.480) \quad (1)$$

where x is the concentration percentage of PTP. This equation may be used with the values of T_g shown in Figure 4(a,b) to assess the distribution of the additives, mainly PTP, the primary solute in the scintillator.

As can be seen in Figure 4(a), for tile 136, T_g of the material is higher than that of the material with an effective concentration of 1.5% PTP and 0.05% POPOP. If such an increase is mainly due to PTP, the average amount of PTP effectively added is about 1.45%. The amount of PTP added, as estimated from eq. (1) and from the T_g data in Figure 4(a), should range between 1.42 and 1.48%.

An opposite behavior was verified for tile 17. In this case, from the T_g data, it is possible to conclude that the incorporation of additives is heterogeneous, varying between 1.52 and 1.12% PTP with an average value of 1.32%. This heterogeneous distribution may be responsible for the poorer optical performance of this tile. This evidence is better illustrated in Figure 6, where the T_g data for both tiles, obtained from scans at 8°C/min, are plotted against the concentration of PTP estimated with eq. (1).

The main difference in the processing conditions of these tiles (Table I) is the back-pressure, the processing variable that influences the homogeneity of mixing, which is 2 MPa for tile 17 and 3 MPa for tile 136. The back-pressure effect, allowing for better homogenization of the dopants in tile 136, results in lower nonuniformity of the light output.

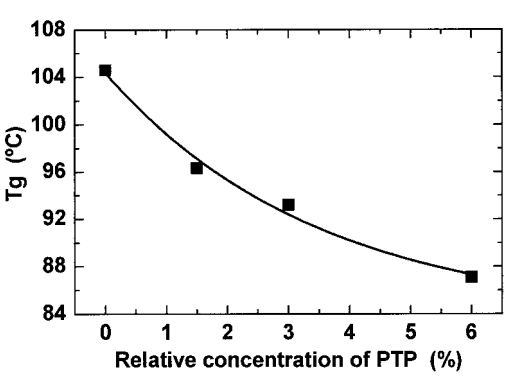

Figure 5 Variation of T_g as a function of the PTP concentration at a scanning rate of 8°C/min.

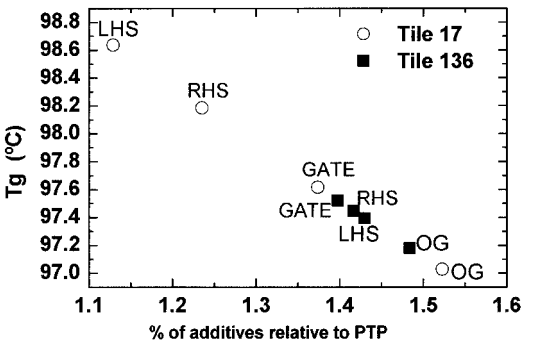

Figure 6 T_g plotted against the percentage of additives relative to PTP at a scanning rate of 8°C/min. The samples were collected from tiles 136 and 17 at the gate, at the opposite side to the gate (OG), at the left-hand side (LHS) of the tile, and at the right-hand side (RHS) of the tile.

CONCLUSIONS

The additives are incorporated into scintillating tiles in smaller amounts than intended. The actual amount incorporated ranges from less than 1% to 9%. An additional amount of the solutes should be added during the mixing process to account for the loss of the additives that adhere to the walls of the mixing barrel when this method of mixing is used.

The heterogeneous distribution of the additives, which may be estimated from the T_g data of samples taken from different parts of the tile, is strongly correlated with poorer optical performance of the tiles, that is, the nonuniformity of the optical yield.

As mentioned elsewhere,[1] in cast-molded scintillators, minor changes in the relative light output have been observed for molecular weights greater than 10^5 g/mol. Apparently, changes by a factor of 100 in the molecular weight do not affect the optical efficiency.

The Atlas project literature[2] states the need for further research and development in the injection-molding processing route to promote the uniformity of the light output and to improve the average light yield of the scintillating tiles. A partial answer to this need is given in this work, which shows that the control of the back-pressure and the use of lower mold temperatures help to promote a better optical performance. This results from an improved homogenization of the molten polymer injected into the tile and from the lower temperatures restraining the migration of the additives. Furthermore, an effective control of the amount of the solutes actually incorporated into the polymer matrix is desirable.

APPENDIX

A scintillation event in a ternary system, X + Y + Z, in which X is the solvent (main constituent) and Y and Z are the primary and secondary solutes, respectively, can be divided into primary and secondary processes. Because the concentrations of the solutes (Y and Z) are small, their direct excitation may be neglected in the primary process. Therefore, at this stage, there is mainly a transfer of energy from the ionizing radiation to the excitation energy of X; the electronically excited states may decay, emitting light. Among the secondary processes, those competing for the excitation energy of X are included: the energy transfer to the molecules of Y and Z, the energy migration to other molecules of X, and the emission as fluorescence.

The absolute scintillation efficiency of a ternary scintillator is

$$S_z \cong 0.1 \cdot Q_z, \tag{A1}$$

where Q_z is the overall efficiency of the secondary processes:

$$Q_z = C \frac{E_{pz}}{E_{lx}} f_{xy} f_{yz} q_{oz} \tag{A2}$$

C is the degree of internal conversion from the mean excitation energy (E_{ex}) of the π singlet states of the X molecules due to the 0.1 fraction of the incident energy into the energy of the first excited π singlet state of X (E_{1x}) with a quantum efficiency of $\bar{q}_{1c}$ [$C = (E_{1x}/E_{ex})\bar{q}_{1c}$]; f_{xy} and f_{yz} are the quantum efficiencies of the energy transfer from X to Y and from Y to Z, respectively; q_{oz} is the fluorescence quantum efficiency of Z; and E_{pz} is the energy at which the fluorescent photons escape from the sample. Because of the radiative migration, E_{pz} is lower than the energy of emission of fluorescent photons from the excited state to the ground state. A detailed analysis of the de-excitation processes competing for energy E_{1x} can be found in ref. 3.

References

1. Martins, J. A.; Seixas, J.; Silva, J.; Esteves, V.; Oliveira, M. J.; Gomes, J.; Maio, A.; Pouzada, A. S. J Appl Polym Sci 2003.
2. Atlas Tile Calorimeter; Technical Design Report CERN/LHC/96-42, Atlas TDR 3; CERN: Geneva, Switzerland, 1996.
3. Birks, J. B. The Theory and Practice of Scintillation Counting; Pergamon: New York, 1964.
4. Senchishin, V. G.; Markley, F.; Lebedev, V. N.; Kovtun, V. E.; Koba, V. S.; Kuznichenko, A. V.; Tizkaja, V. D.; Budagov, J. A.; Bellettini, G.; Seminozhenko, V. P.; Zalubovsky, I. I.; Chirikov-Zorin, I. E. Nucl Instrum Methods Phys Res Sect A 1995, 364, 253.
5. Yoshimura, Y.; Inagaki, T.; Moromoto, T.; Sugai, I.; Kuriki, M.; Shirai, R.; Goto, M.; Yamashina, T. Nucl Instrum Methods Phys Res Sect A 1998, 406, 435.
6. Nemashkalo, A.; Popov, V.; Rubashkin, A.; Sorokin, P.; Zatserklianiy, A.; Borishenko, A.; Senchishin, V.; Skrebtsov, O.; Bolotov, V. Nucl Instrum Methods Phys Res Sect A 1998, 419, 609.
7. Swank, R. K.; Buck, W. L. Phys Rev 1953, 91, 372.